

A simple graphical method for the analysis of the selective population transfer in many-level quantum systems

D. Bonacci²

Department of Physical Chemistry, R. Boskovic Institute, Bijenicka 54, 10000

Zagreb, Croatia

E-mail: dbonacci@irb.hr

Abstract

Controlled manipulation of the quantum systems is becoming an important technological tool. Rabi oscillations are one of the simplest, yet quite useful mechanisms for achieving such manipulation. However, the validity of simple Rabi theory is limited and its upgrades are usually both technically involved as well as limited to simple two-level systems. The aim of the paper is to demonstrate a simple graphical method for the analysis of the applicability of simple Rabi solutions to the controlled population transfer in complex multi-level quantum systems.

I Introduction

State selective manipulation of discrete-level quantum systems such as atoms, molecules or quantum dots is the ultimate tool for many diverse fields such as laser control of chemical reactions, atom optics, high-precision metrology and quantum computing [1]. The elementary process on which many of the schemes of such manipulation rely are 'Rabi' population oscillations between two selected levels of the system. In the lowest approximation these oscillations are induced by perturbing the system with the coherent monochromatic force tuned into resonance with the desired transition. The name of this phenomenon stems from the name of the author of the first approximate analytic assessment of this process [2].

Original Rabi theory is simple to present and comprehend, but has two drawbacks. First is that due to the rotating wave approximation (RWA), under which it is obtained, its validity is limited even in the pure two-level systems. A number of papers has been published concerning the solution to the population dynamics without RWA (e.g. [3,4,5]) which are all based on high-level mathematical apparatus and hence quite un-intuitive. Also, as these methods are founded on the perturbative approaches, the solution in the case of the extreme breakdown of the RWA - which is extremely simple (although maybe not very useful) - is seldom described. Second, analytical approach to the single-laser Rabi oscillations is generally constrained to simple two level

system, and hence its validity is necessarily limited when it is applied to more complex multi-level systems. Since many (or, indeed, most...) interesting real systems actually are multi-level systems, at least a rough assessment of the influence of their structural complexity on Rabi oscillations between selected two levels should be done before applying them to complex systems.

In this paper both these questions are addressed. In the first section mathematically simple, yet thorough analysis of the limitations of the RWA approximation in two-level systems is presented. In the second a simple graphical criterion (based on Rabi profiles) for the analysis of validity of the RWA-based solutions is established. This enables quick estimation of the validity of the Rabi solution for certain system parameters just by visually inspecting the shape of simple Lorentzian curve. Finally, third section is devoted to discussion of how Rabi profiles may be used to estimate the validity of the two-level Rabi solution in the general multi-level system.

Although presented analysis is graphical – and hence not very strict in mathematical sense – it is nevertheless firmly anchored with solid analytically established arguments. It enables very good order-of-magnitude estimates of the maximum driving field intensities that can be used to efficiently drive the selected transition. Most of all, it offers conceptual simplicity and intuitiveness which are both of utmost importance when the whole subject is presented either to interested non-experts or to the newcomers in the field. Hence we consider it very suitable as both quick lab-reference tool as well as the simple

didactic introduction into much more involved strict quantitative theory.

In all calculations the value of the Planck constant is taken to be $\hbar = 1$.

II Rotating wave approximation in the two-level system

In this section a simple, yet thorough analysis of the validity of Rabi RWA solution in the two level system is presented. The results obtained – majority of which are quite well known – will serve as the strict mathematical basis for the consequent discussions.

II.1 Full dynamical equation

Consider the two-level quantum system. Its dynamics is described by the time dependent Schrodinger equation:

$$i \frac{\partial}{\partial t} \psi(\mathbf{x};t) = (H_0(\mathbf{x}) + V(t)) \psi(\mathbf{x};t); \quad (1)$$

\mathbf{x} denotes the set of all the spatial coordinates of the system. $H_0(\mathbf{x})$ is the unperturbed time-independent Hamiltonian of the system, satisfying the eigenequation:

$$H_0 \psi_i(\mathbf{x}) = E_i \psi_i(\mathbf{x}) ; (i = 1;2); \quad (2)$$

where $\psi_i(\mathbf{x})$ and E_i are eigenfunctions and respective total energies of the unperturbed system. $V(\mathbf{x};t)$ is the homogeneous monochromatic perturbation:

$$V(\mathbf{x};t) = \hat{V}(\mathbf{x})F_0 \cos(\omega t); \quad (3)$$

$\hat{V}(\mathbf{x})$ is the spatial operator odd with respect to central inversion (e.g. dipole, quadrupole, ...) through which the perturbation establishes coupling between the two levels of the system. F_0 is the parameter determining the perturbation intensity (which shall be referred to as the perturbation intensity for short). ω is constant tunable frequency of the external perturbation. Expressing the solution $\psi(\mathbf{x},t)$ as an expansion over eigenstates $\psi_i(\mathbf{x})$,

$$\psi(\mathbf{x},t) = \sum_{i=1}^{\infty} a_i(t) \psi_i(\mathbf{x}) e^{-iE_i t}; \quad (4)$$

Eq. (1) transforms into a system of two coupled differential equations for the time dependent expansion coefficients $a_i(t)$:

$$\frac{d}{dt} a_j(t) = -iF_0 \cos(\omega t) \sum_{i=1}^{\infty} a_i(t) I_{ij} e^{i(s_{ij} - \omega) t}; \quad (j = 1;2); \quad (5)$$

Here $s_{ij} = s_{ji} = \text{sign}(\omega_{ij})$, $\omega_{ij} = E_j - E_i$ and $I_{ij} = \int \psi_i(\mathbf{x}) \hat{V}(\mathbf{x}) \psi_j(\mathbf{x}) dx$.

From the definition it is evident that $I_{12} = I_{21}$ and $I_{11} = I_{22} = 0$. Combining the two expansion coefficients into a two-component vector $\mathbf{a}(t)$, expanding a cosine term as $\frac{e^{i\omega t} + e^{-i\omega t}}{2}$ and re-scaling the time variable to

$$\mathbf{a}_2 \frac{F_0 I_{12}}{2} t \quad (6)$$

casts Eq. (5) into convenient matrix form :

$$\frac{d}{dt} \mathbf{a}(t) = \begin{bmatrix} 0 & e^{2i} + e^{-2i} \\ e^{-2i} + e^{2i} & 0 \end{bmatrix} \mathbf{a}(t); \quad (7)$$

where $\frac{1}{F_0 I_{12}}$ and $\frac{1 + I_{12}}{F_0 I_{12}}$.

Evolution of the population of particular level is given by $n_i(t) = |a_i(t)|^2$.

II.2 RWA solution and its limitations

Rotating wave approximation hinges on the assumption that the complex exponential terms containing $e^{\pm 2i}$ in Eq. (7) have only minor (or even negligible) impact on the system dynamics and may hence be dropped in all further calculations. However, in order to fully explore their influence, they shall be kept throughout this calculation.

Now the following procedure is administered: first Eq. (7) is differentiated with respect to t ; then the same equation is used to eliminate the $\frac{da_i(t)}{dt}$ that appears during differentiation on the right-hand side; finally the matrix equation is split into two ordinary coupled differential equations for coefficients $a_1(t)$ and $a_2(t)$. The following expression is hence obtained:

$$\frac{d^2}{dt^2} a_{1,2}(t) = \begin{bmatrix} 2a_{1,2}(t) & e^{2i} a_{2,1}(t) \\ e^{-2i} a_{2,1}(t) & 2 \cos(2(\omega + \phi)) a_{1,2}(t) \end{bmatrix}; \quad (8)$$

where first index corresponds to the upper sign and second to the lower. As

no approximations have yet been introduced, this is still the full dynamical equation equivalent to Eq. (7). Initial conditions comprise the whole population of the system located in one of the two levels, with the other level being completely empty.

Keeping only the first term on the right-hand side of the Eq. (8) leads straight to the on-resonance Rabi solution, sinusoidal population oscillations with period $T_0 = \frac{1}{\Omega}$ and amplitude $A_0 = 1$ (for details see e.g. [6]). Whether or not the remaining terms on the right-hand side may be considered dynamically insignificant depends on the relation between period T_0 and the periods of the oscillating and complexly rotating parts of these remaining terms. If any of those is much smaller than T_0 then the value of the elements on the right-hand side in which they are contained averages up to zero during any time interval small compared to one in which $a_1(\omega)$ and $a_2(\omega)$ significantly change, and hence they play no dynamical role. Otherwise they have to be taken into consideration.

As ϵ can be reduced at will to any small value (or indeed to zero), the period of the second term in Eq. (8) can be reduced to any small value, so this element cannot be dropped at all. Taken together, first two terms lead to the 'generalized' Rabi oscillations with period $T = \frac{1}{\Omega \sqrt{1 + \frac{\epsilon^2}{4}}}$ and amplitude $A = \frac{1}{\sqrt{1 + \frac{\epsilon^2}{4}}}$ (for details see e.g. [6]). So, the shift from resonance increases the frequency of the population oscillations but at the same time reduces their amplitude.

Third term in Eq. (8) regulates the additional 'Bloch-Siegert' oscillations superimposed on the pure sinusoidal population transfer curve. They are caused by the non-neglected complex exponentials containing ω in Eq.(7), and cause the shift in the resonant frequency ω_{12} ([7]). Based on the previously discussed argument we expect that it may be neglected if $\omega \gg 1$. However, as ω can be quite large and it provides the amplitude to the rotating complex exponential, it would be useful to quantify this argument and calculate exactly what the amplitude of these superimposed population oscillations is. The corrected solution is sought as a sum $a_0(t) + a_1(t)$ where $a_0(t)$ is the generalized Rabi RWA solution and $a_1(t)$ the correction. Inserting this sum into Eq. (7) and assuming that $a_0(t) \gg a_1(t)$ componentwise, the formal solution for the correction is obtained

$$a_1(t) = \frac{1}{i} \int_0^t \left[\frac{\Omega}{2} e^{2i\omega t'} a_0(t') - \frac{\Omega}{2} e^{-2i\omega t'} a_0(t') \right] dt' \quad (9)$$

If $\omega \gg 1$, frequency of $a_1(t)$ will certainly be much smaller than the frequency of the complex exponentials inside the matrix. Hence we can evaluate the obtained integral between some t_0 and $t_0 + \Delta t$ such that $\Delta t \ll 1/\omega$ by taking the almost constant $a_0(t) \approx a_0(t_0)$ outside the integral sign. Remaining integration is simple and it finally yields

$$a_1(t) = \frac{1}{i} \frac{\Omega}{4} \frac{e^{2i\omega t} - e^{2i\omega t_0}}{2} - \frac{\Omega}{4} \frac{e^{-2i\omega t} - e^{-2i\omega t_0}}{2} a_0(t_0) \quad (10)$$

Frequency of the components of $a_1(t)$ is evidently much higher than that

of the corresponding components of $a_{1,2}(\omega)$. As the amplitude of both matrix elements is 1, the ratio of the amplitudes of the correction components and the generalized Rabi-RWA solution components $\frac{a_{1,2}(\omega)}{a_{1,2}(\omega)}$ amounts $\frac{1}{2}$. Thus indeed while $\omega \gg 1$, $a_{1,2}(\omega) \gg a_{1,2}(\omega)$ and hence the third term in Eq. (8) may be neglected.

The last remaining term in Eq. (8) has fixed amplitude equal to 4. It can be neglected if $\omega + \Omega \gg 1$, and since Ω can be reduced to zero, in the worst case this reduces to $\omega \gg 1$ - which is the same as for the third component. However, this term has a prominent role in the extreme situation, when $\omega < 1$. In such case third term may be neglected due to its vanishing amplitude, and since $\omega < \Omega$ even more so may the second term. Eq. (8) then reduces to

$$\frac{d^2}{dt^2} a_{1,2}(\omega) = 2[1 + \cos(2(\omega + \Omega)t)] a_{1,2}(\omega) \quad (11)$$

which leads to the population oscillations with amplitude 1, but with temporally modulated period $T(\omega) = \frac{1}{\omega + \cos(2(\omega + \Omega)t)}$. As with the third term, it is inherently related to the inclusion of the 'non-RWA' contributions in matrix in Eq. (7). It should be kept in mind that in this case the perturbation is extremely strong. Under such circumstances the corresponding potential $V(t)$ in dynamical equation (Eq. (3)) might need to be corrected with higher order interaction terms (quadrupole, octupole,...). Indeed, it may also happen that the structure of the original two-level system becomes significantly distorted or even that the system breaks up completely. Hence this result might not be

very useful from the point of controlled system manipulation.

All in all, it may be concluded that Rabi-RWA solution is excellent approximation to the exact solution of Eq.(7) in the complete spectral range $0 < \omega < \omega_{12}$ - and not just close to resonance ω_{12} - of perturbation frequencies as long as

$$\omega \gg \omega_{12} \quad (12)$$

III Graphical analysis using Rabi profiles

In this section the notion of Rabi profile is introduced and it is demonstrated how the obtained condition for the validity of the Rabi-RWA solution, $\omega \gg \omega_{12}$, can conveniently be visualized in terms of it.

III.1 Rabi profile of a single system transition

Rabi profile of the transition between levels 1 and 2 simply refers to the amplitude of population oscillations exhibited by the generalized Rabi-RWA solution, considered as a function of the driving frequency ω . It is parameterized with total coupling strength (or coupling) $D_{12} = F_0 I_{12}$ and resonant frequency of the system ω_{12}

$$P_{12}(\omega) = \frac{1}{1 + \frac{(\omega - \omega_{12})^2}{D_{12}^2}} \quad (13)$$

As can be seen from the Fig. 1, it is a simple bell-shaped curve centered on ω_{12} with half-width at half-maximum (or half-width) equal to D_{12} .

Expressing the condition (12) in terms of the drive frequency, resonant transition frequency and coupling we obtain a simple criterium for estimating the validity of a generalized Rabi-RWA solution in the particular two-level system driven by the external homogeneous coherent perturbation: $D_{12} \ll \omega_{12} + \omega$.

In the worst case this reduces to

$$D_{12} \ll \omega_{12} \quad (14)$$

or, put in words, distance of the probe's center from the origin of the spectrum ($\omega = 0$) must be much greater than the probe's half-width. We may also rephrase it as: 'At the origin of the spectrum the height of the probe must be negligible'. If this condition is fulfilled, population of a two-level system driven with any desired frequency ω will exhibit pure sinusoidal oscillations with amplitude equal to the height $P_{12}(\omega)$ of the Rabi probe at the selected frequency and period equal to

$$T_{12}(\omega) = \frac{\pi}{D_{12}} P_{12}(\omega) \quad (15)$$

Fig. 2 exhibits four cases of population dynamics in the resonantly driven two-level system. These are obtained as the 'exact' numerical solution to Eq. (7). Four presented cases respectively correspond to the Rabi probes in Fig. 1, as indicated with value of coupling D_{12} above each graph. In the first case,

the coupling is relatively weak so that the condition (12) is fully satisfied (actually, $\epsilon = 50$) and pure sinusoidal population oscillations are observed. The second case is a limiting one ($\epsilon = 5$): a minor rapidly oscillating Bloch-Siegert component may be observed superimposed on top of the major sinusoidal oscillations. In the third case $\epsilon = 1$ so that major discrepancy from the sinusoidal oscillations is expected, and is indeed observed, with the Bloch-Siegert and Rabi components being roughly of the same order of magnitude. The last case ($\epsilon = 0.1$) corresponds to lower limit of the extreme coupling ($\epsilon \ll 1$), and as predicted, the quasi-sinusoidal oscillations with time-dependent period are observed.

Fig. 3 displays the numerical solutions for the population dynamics of two-level systems driven by the off-resonant perturbation. The Rabi profile (displayed in the top graph) is the same in all four cases, with resonant frequency equal to $\omega_{12} = 1$ and coupling equal to $D_{12} = 0.05$. By visual inspection it may be checked that the condition for validity of the Rabi-RWA solution is fulfilled, while analytically it amounts to $\epsilon \gg 20$. The four perturbation frequencies ($\omega_a = 1.050$, $\omega_b = 0.850$, $\omega_c = 0.503$ and $\omega_d = 2.580$) are chosen so that $P_{12}(\omega_a) = 0.5$, $P_{12}(\omega_b) = 0.1$, $P_{12}(\omega_c) = 0.01$ and $P_{12}(\omega_d) = 0.001$. Vertical gridlines are drawn at the integral multiples of the predicted population oscillation time determined from (15). Horizontal gridlines are drawn at the predicted Rabi-RWA value of the population oscillation amplitude. In the case a. the observed dynamics are clearly sinusoidal oscillations with the predicted

amplitude and period. In the case b. the excellent agreement between the predicted Rabi Ω values and the numerical results is also clear. However, the minor Bloch-Siegert oscillations of amplitude $\frac{1}{2} \approx 0.05$ may be noted. In the case c. again the predictions are quite fair, although the amplitude of the Bloch-Siegert oscillations is now of the same order as the Rabi component so the dynamics is not purely sinusoidal, but is rather doubly periodic. In the last case, d. situation is similar to the one in case c., but as Ω is somewhat larger for this case, the agreement is somewhat better. Altogether, the usefulness of the graphical criterium is clearly confirmed. With narrower profiles situation is even better.

III.2 Multi-level system and Rabi spectrum

As a first instance of multi-level system a three-level one shall be considered. It is actually the most important example, as all the consequent conclusions on the behavior of the many-level systems are a mere generalization of the findings from a three-level case. Let the internal structure of this system be such that drive couples level 1 to level 2 with total strength $D_{12} = F_0 I_{12}$ and level 2 to level 3 with total strength $D_{23} = F_0 I_{23}$, but does not couple level 1 directly to level 3 (i.e. $I_{13} = 0$). The spectrum of the system hence contains two resonant frequencies, ω_{12} and ω_{23} . Initially let the whole population be located in level 2. The main goal is to transfer it to the level 1 minimizing both the transfer time and the losses to the level 3. Based on the results discussed in

the previous section the dynamics of the three-level system might be predicted to some extent by inspecting the common plot of the two Rabi profiles $P_{12}(\omega)$ and $P_{23}(\omega)$ (top graphs in Figures 4, 5 and 6). Such plot containing all the Rabi profiles of the spectral lines which couple any of the two targeted levels (1 and 2 in this case) among themselves and to the rest of the system (just level 3 in this case) shall be referred to as the Rabi spectrum of the particular targeted transition.

Assume that both profiles are 'narrow' so that for both of them Eq. (14) holds. Further assume that both profiles are also 'narrower' then the distance between their centers, $|j_{12} - j_{23}| \gg D_{12}; D_{23}$. This situation is displayed on top graph in Figure 4, and it can always be achieved by sufficiently reducing the drive intensity, F_0 . Now consider each of the two transitions separately. Consider tuning the perturbation to ω_{12} . As $P_{12}(\omega_{12}) = 1$ and $P_{23}(\omega_{12}) \ll 1$, such perturbation would induce the complete population transfer oscillations on transition 1 \leftrightarrow 2 and almost negligible population oscillations on transition 2 \leftrightarrow 3. Hence, if such a drive is applied to the three-level system, it might be expected that it would indeed produce complete population oscillations between levels 1 and 2 and would have almost negligible effect on the level 3. Validity of this prediction can be clearly observed by inspecting the numerical solution presented in the bottom graph of Figure 4.

According to Eq. (15), an increase in the speed of population transfer can be achieved by increasing the coupling through increasing the perturbation

intensity F_0 . Suppose that system parameters (resonant frequencies and coupling integrals) are such that after the drive intensity is increased both profiles still satisfy Eq. (14), but that now the profile of the undesired transition 2-3 broadens to such an extent that $P_{23}(\omega_{12})$ is still small but not negligible anymore. This situation is displayed on the top graph of the Figure 5. Considering again each transition by itself, drive with frequency (ω_{12}) would again produce the complete periodic population transfer on transition 1-2, but would also produce a clearly observable - albeit not complete - population oscillations on 2-3. So in the three level system we expect the population dynamics would change from that in the previous case as now both transitions 'react' significantly to the applied drive. Based on the discussion in the previous section, it can be suggested that it would roughly comprise of most population being exchanged along transition 1-2 with the remaining fraction being now also exchanged among levels 2 and 3. This is clearly observed from the numerical solution displayed on the bottom graph of Figure 5. It can also be observed that the maximum amplitude of the perturbing level's equals almost exactly $P_{23}(\omega_{12})$.

By further increasing the perturbation intensity (Figure 6) the simple sinusoidal pattern of oscillations on the transition 1-2 disappears completely. Hence the perturbation this strong cannot be employed to drive the efficient population transfer along the transition 1-2. This suggests that in a general many-level quantum system there is an upper limit to speed of the efficient

population transfer (i.e. such that great majority of the population is transferred) along each particular transition. This limit is determined exclusively by the internal properties of the system. Consider two levels $|g\rangle$ and $|e\rangle$ of a many-level system that are directly coupled by the applied drive, i.e. such that $I \neq 0$. The efficient transfer along transition $|g\rangle \rightarrow |e\rangle$ is feasible as long as none of the profiles from that particular transition's Rabi spectrum has significant height at the resonant frequency of that transition – except, of course, the Rabi profile of that selected transition (which is 1 at its own resonant frequency). Certainly, it should also be kept in mind that the Rabi profile of that selected transition has to have negligible height at the origin.

IV Conclusions

First hint of the method presented in this paper that we are aware of appeared quite some time ago in [8]. Several graphs in that paper are exact equivalents (actually, antecedents) of Rabi spectra, but there their usefulness has passed unnoticed. Although the method is quite simple, it does offer some guidelines for one interesting application. Namely, knowing the details of the internal structure of a particular quantum system, we can easily calculate Rabi spectrum for each transition in that system. We can then use this data to quickly quantitatively estimate the lower limit for the clean population transfer time that can be achieved on any particular transition. Finally we can build a nu-

merical scheme to search for the quickest pathway through the system along which the population can be transferred between any two selected levels, and give the lower limit of the time needed.

Full analytical treatment of the selective population transfer mechanism provides us with many additional interesting results. It can thus be shown ([9,10]) that by using analytically determined chirp (i.e. time dependent variation of the perturbation frequency) instead of resonant frequency to drive any particular transition, much more efficient population transfer can be achieved.

| | | | | | | | | | | | | | | | | | |

References

- [1] C.H. Bennett, D.P. DiVincenzo, Quantum information and computation, Nature 404 (2000) 247-255.
- [2] I. Rabi, Space quantization in a gyrating magnetic field, Phys. Rev. 51 (1937) 652-654.
- [3] M.S. Shariar, P.P. Radhan, Fundamental limitation on qubit operations due to the Bloch-Siegert oscillation, Proceedings of the quantum communication, measurement and computing (QCMC'02) Quant-ph/0212121.
- [4] J.C.A. Barata, W.F. Wreszinski, Strong coupling theory of two level atoms in periodic fields, Phys. Rev. Lett. 84 (10) (2000) 2112-2115, quant-ph/9906029.

- [5] K Fujii, Two-level system and some approximate solutions in the strong coupling regime Quant-ph/0301145.
- [6] W Demtroeder, Laser spectroscopy: basic concepts and instrumentation, 1st Edition, Springer-Verlag, Berlin, 1988.
- [7] F Bloch, A J F Siegert, PhysRev. 57 (1940) 522.
- [8] M Quack, E. Sutcliffe, Primary photophysical processes in infrared multiphoton excitation: wavepacket motion and state selectivity, Infrared Physics vol25 (1-2) (1985) 163{173.
- [9] D Bonacci, Analytic pulse design for selective population transfer in many-level quantum systems: maximizing the amplitude of population oscillations (in preparation).
- [10] D Bonacci, Analytic pulse design for selective population transfer in many-level quantum systems: fixing pulse duration (in preparation).

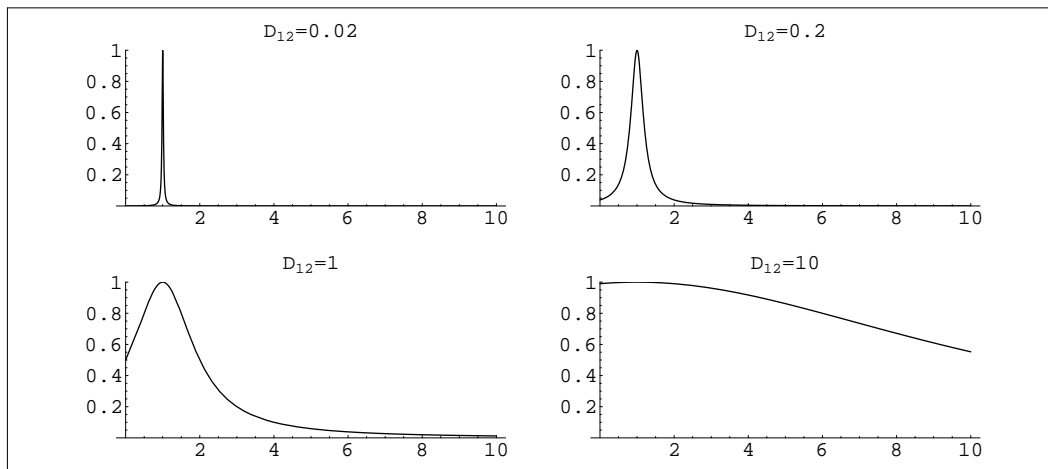


Figure 1. Rabi profiles of a single spectral line. On all graphs abscissa is ω and ordinate is $P_{12}(\omega)$. In all cases the resonant frequency is $\omega_{12} = 1$ and respective couplings D_{12} are indicated above each graph. Both quantities are expressed in terms of relative units of resonant frequency. Observe how the profile's halfwidth increases with increasing coupling.

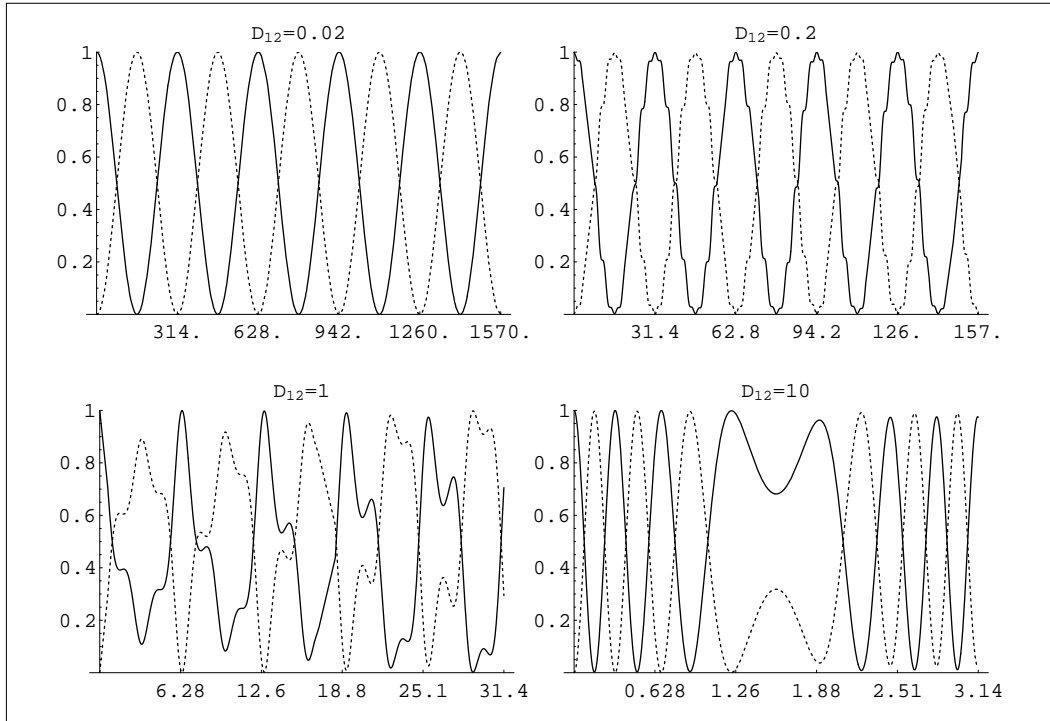


Figure 2. Exact numerical solution for population dynamics of the two-level system subjected to resonant perturbation. On all graphs abscissa is t and ordinate is $\rho_{1,2}(t)$. Initially the complete population is located in level 1. Populations $\rho_1(t)$ and $\rho_2(t)$ are respectively represented with full and dotted lines. Tick-marks are located at integral multiples of population transfer period calculated from Eq. (15) corresponding to the respective value of D_{12} .

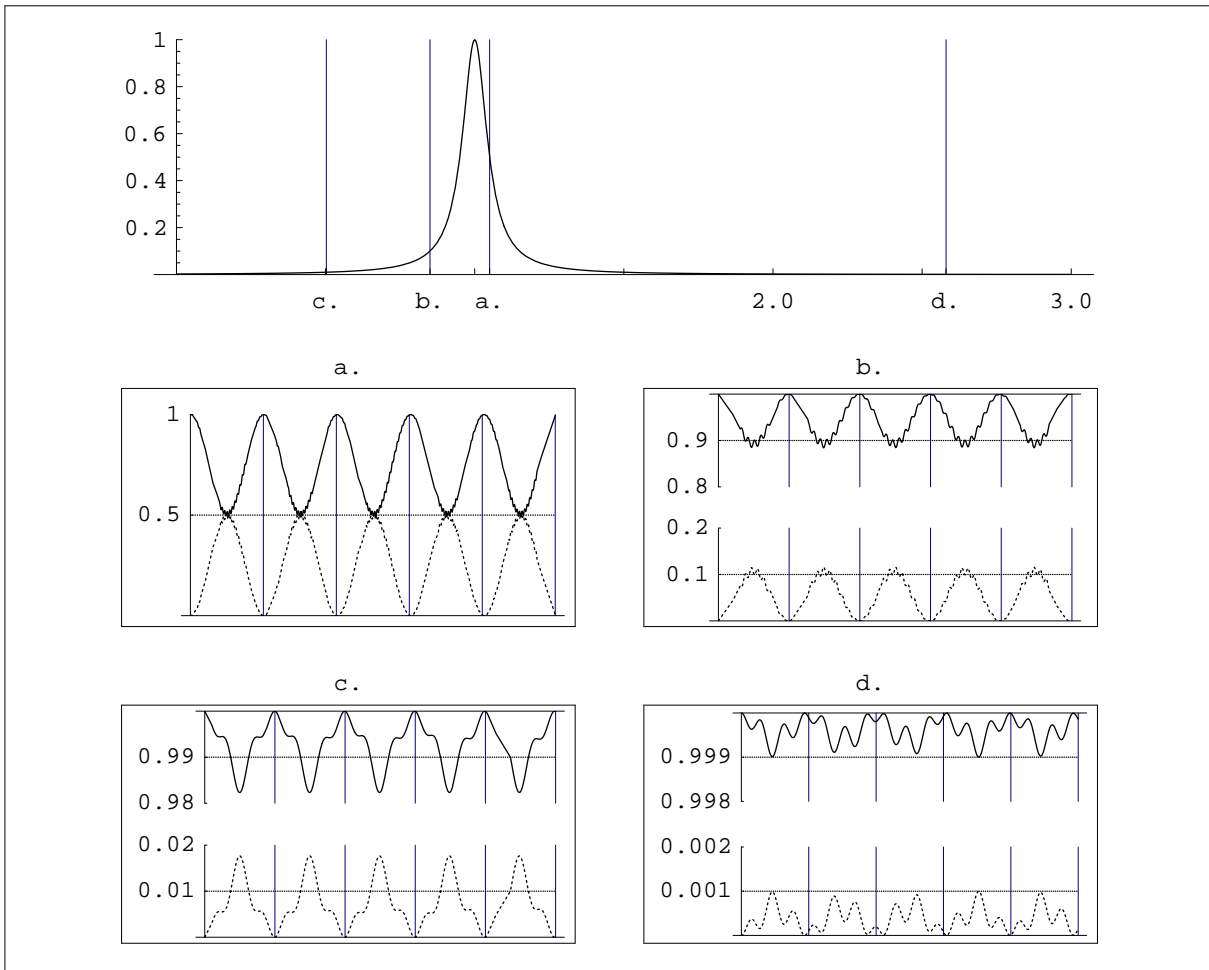


Figure 3. Numerical solutions for the population dynamics of the two-level system subjected to non-resonant perturbations. On the top graph the common Rabi profile is displayed, with Δ on the abscissa and $P_{12}(\Delta)$ on the ordinate. Vertical lines indicate the different perturbation frequencies for each of the four cases presented. Letters under the lines indicate which dynamics graph corresponds to each perturbation. On four bottom graphs the population dynamics is displayed, with t on the abscissa and $P_{1,2}(t)$ on the ordinate. Time t and frequency Δ are given in relative units.

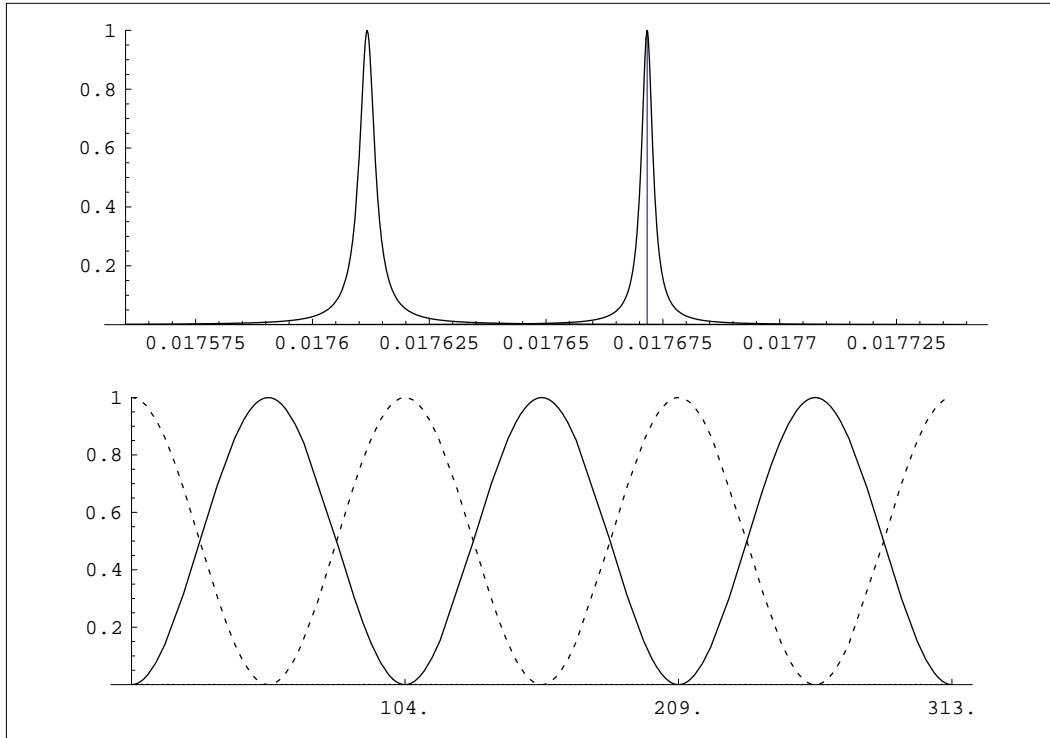


Figure 4. Rabi spectrum and numerical solution for the population dynamics of a three-level system. On the top graph the two Rabi profiles corresponding to the two resonant lines of the system are plotted alongside. Abscissa is ω (atomic units) and the ordinate is $P_{12,23}$ (!) (no units). Perturbation frequency is indicated with the vertical line on the Rabi spectrum plot, and it is set to the resonant frequency ω_{12} . Bottom graph presents the population dynamics of all three populations. Full line is $n_1(t)$, dashed line is $n_2(t)$. Population of the level 3 would be drawn as the dotted line, but it is so negligibly small at all times that it cannot be distinguished from the x-axis. Abscissa is t (ns) and ordinate is $n_{1,2,3}(t)$.

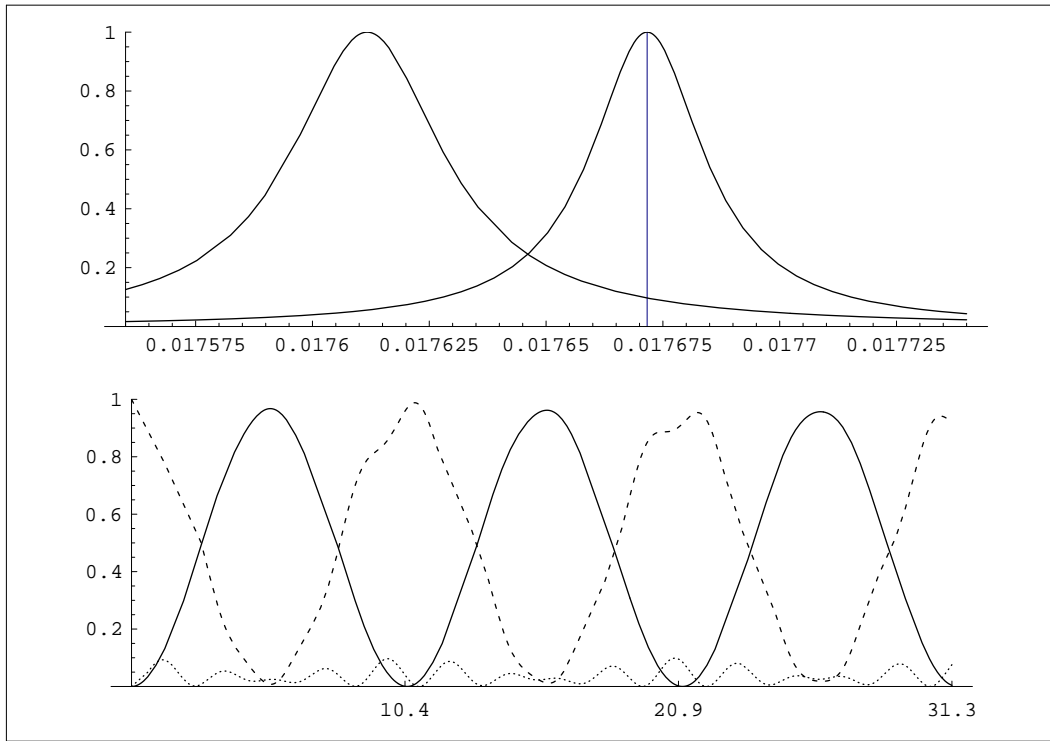


Figure 5. Rabi spectrum and numerical solution for the population dynamics of a three-level system. On the top graph the two Rabi profiles corresponding to the two resonant lines of the system are plotted alongside. Abscissa is ω (atomic units) and the ordinate is $P_{12,23}(\omega)$ (no units). Perturbation frequency is indicated with the vertical line on the Rabi spectrum plot, and it is set to the resonant frequency ω_{12} . Bottom graph presents the population dynamics of all three populations. Full line is $P_1(t)$, dashed line is $P_2(t)$ and dotted line is $P_3(t)$. Abscissa is t (ns) and ordinate is $P_{1,2,3}(t)$.

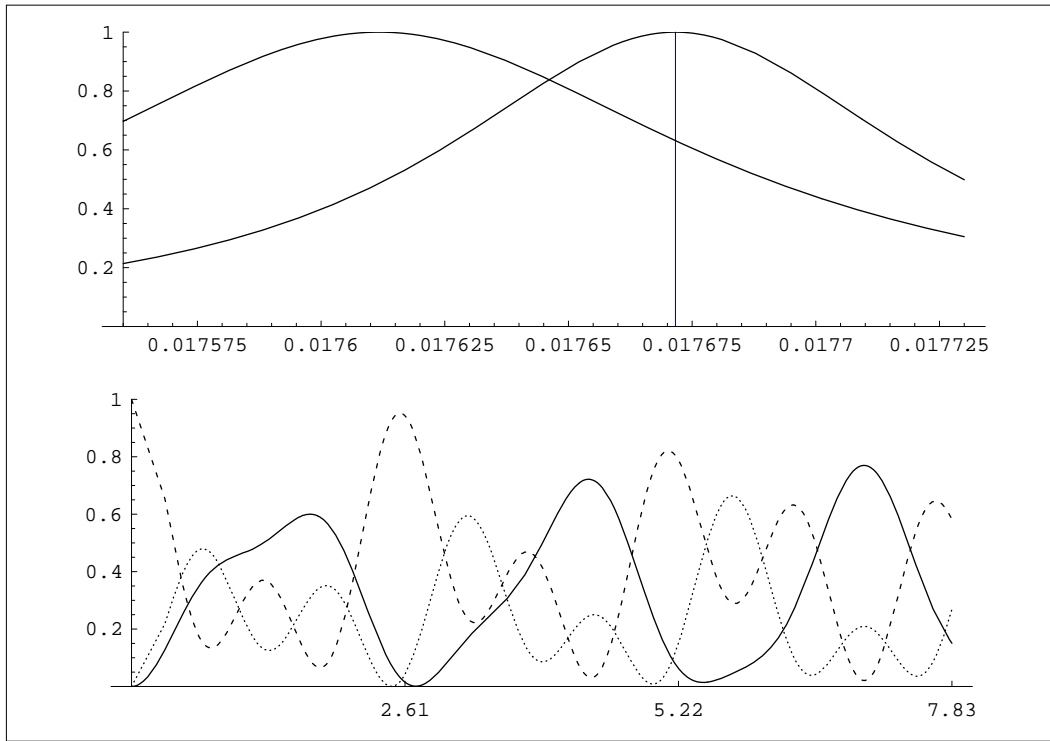


Figure 6. Rabi spectrum and numerical solution for the population dynamics of a three-level system. On the top graph the two Rabi profiles corresponding to the two resonant lines of the system are plotted alongside. Abscissa is ω (atomic units) and the ordinate is $P_{12,23}(\omega)$ (no units). Perturbation frequency is indicated with the vertical line on the Rabi spectrum plot, and it is set to the resonant frequency ω_{12} . Bottom graph presents the population dynamics of all three populations. Full line is $\rho_{11}(t)$, dashed line is $\rho_{22}(t)$ and dotted line is $\rho_{33}(t)$. Abscissa is t (ns) and ordinate is $\rho_{1,2,3}(t)$.